Spin-Density-Wave Antiferromagnetism of Cr in Fe/Cr(001) Superlattices

Eric E. Fullerton and S. D. Bader

Materials Science Division, Argonne National Laboratory, Argonne, Illinois 60439-4845

J. L. Robertson

Solid State Division, Oak Ridge National Laboratory, Oak Ridge, Tennessee 37831-6393

(Received 22 November 1995)

The antiferromagnetic spin-density-wave (SDW) order of Cr layers in Fe/Cr(001) superlattices was investigated by neutron scattering. For Cr thicknesses from 51 to 190 Å, a transverse SDW is formed for all temperatures below the Néel temperature with a single wave vector $\mathbf{Q}$ normal to the layers. A coherent magnetic structure forms with the nodes of the SDW near the Fe-Cr interfaces, and the magnetic coherence length greater than the Cr layer thickness. The results and modeling provide a direct confirmation of the persistence of bulklike antiferromagnetic SDW order in the Cr. [S0031-9007(96)00855-1]

PACS numbers: 75.70.Cn, 75.25.+z, 75.50.Ee

The magnetic structure in confined geometries of itinerant systems with long-period bulk ordering is a topic ripe for exploration. Cr interleaved in Fe/Cr superlattices is one such system. Bulk Cr is an itinerant antiferromagnet (AF) which forms an incommensurate spin-density-wave (SDW) below its Néel temperature (T_N) of 311 K [1]. The SDW is characterized by a wave vector $\mathbf{Q}$ determined by the nesting of the Fermi surface along the $\langle 100 \rangle$ directions. The Cr spins $\mathbf{S}$ are transverse to $\mathbf{Q}$ ($\mathbf{S} \perp \mathbf{Q}$) above the spin-flip temperature $T_{SF} = 123$ K, and rotate 90° to form a longitudinal SDW ($\mathbf{S} \parallel \mathbf{Q}$) for $T < T_{SF}$. Recent interest has focused on the AF order of thin Cr layers in proximity to Fe [2–9] and its interplay with the biquadratic and oscillatory interlayer coupling of Fe/Cr/Fe sandwiches and superlattices [10–14]. For the thinnest Cr films deposited on Fe(001), the expected Cr AF order is absent due to intermixing and roughness [3,15], and coupling of the initial Cr layers is antiparallel to the Fe [2–7]. For thicker Cr films on Fe(001), two-monolayer (ML) oscillations in the surface-terminated ferromagnetic layer of Cr have been observed [2–4]. Reference [2] further identifies the periodic phase slips in the Cr AF ordering resulting from the incommensurability of the SDW. For sputtered epitaxial Fe/Cr(001), superlattices T_N, identified via transport and magnetic anomalies, are suppressed for Cr thicknesses $t_{Cr} < 42$ Å [13]. For $t_{Cr} > 42$ Å, T_N initially rises rapidly and then asymptotically approaches the value observed in thick Cr films. Recent perturbed-angular-correlation spectroscopy (PACS) measurements for Fe/Cr(001) superlattices grown by molecular beam epitaxy report suppression of AF order for $t_{Cr} < 60$ Å [14].

In this Letter we use neutron diffraction to directly measure the AF-SDW of Cr layers in Fe/Cr(001) superlattices. T_N is found to be strongly thickness dependent and in quantitative agreement with previous transport results [13]. For $t_{Cr} > 50$ Å we find that a *transverse* SDW is formed for all temperatures below T_N, with a single $\mathbf{Q}$ normal to the layers. The SDW period we determine is close to the bulk value, and the magnetic coherence length ξ_m is $> t_{Cr}$ for all samples studied. For $t_{Cr} \leq 44$ Å the neutron scattering results are consistent with commensurate AF order.

Epitaxial Fe/Cr(001) superlattices were grown by dc magnetron sputtering onto 2.5×2.5 cm^2 single-crystal MgO(001) substrates. A 180 Å Cr(001) buffer layer was deposited at 600 °C onto the MgO. The Fe and Cr superlattice layers were deposited at 100 °C. Superlattices grown under these conditions exhibit the expected long-period coupling oscillations and magnetoresistance values as large as 150% [16]. The Fe thickness was held constant at 14 Å for each sample and t_{Cr} was varied from 190 to 31 Å. The number of bilayers was adjusted so that the total Cr thickness is ≥ 1 μm. The superlattice structure was characterized by x-ray diffraction to confirm the (001) epitaxial growth. Multiple superlattice peaks are observed about the Fe/Cr(002) reflections for all of the samples. The crystalline coherence lengths are ≥ 1500 Å and the (002) rocking-curve widths are $\leq 0.7°$ for all samples, except the 44 Å sample whose rocking curve width is 2°. Fitting the x-ray diffraction intensity for the $t_{Cr} = 115$ Å sample yields an Fe lattice spacing of $1.435 + 0.010$ Å, and a Cr spacing of 1.446 ± 0.003 Å indicating a $\approx 0.25\%$ out-of-plane expansion relative to bulk Cr.

Neutron diffraction measurements were performed on the HB-2 and HB-1A triple-axis spectrometers at the HFIR reactor at Oak Ridge National Laboratory. The neutron wavelength was 2.353 Å. Initial temperature-dependent measurements ($T = 12–300$ K) were made on the HB-2 spectrometer using a focused Si(111) monochromator. Subsequent low-temperature measurement were made on the HB-1A spectrometer using a double-crystal graphite (002) monochromator with a pyrolytic graphite filter to suppress harmonic contamination. A graphite (002) analyzer crystal was used for all experiments.

Magnetic scattering from the SDW results in satellites at the Cr $(0, 0, 1 \pm \delta)$ positions [1,17]. The incommensurability δ is given by $1 - aQ/2\pi$, where $a = 2.884$ Å is the Cr lattice constant. In bulk Cr, δ varies continuously from 0.037 at T_N to 0.049 at 10 K, corresponding to SDW periods (a/δ) of 78 and 59 Å, respectively. Shown in Fig. 1 are low-temperature neutron scans about the Cr(001) position for the 115, 63, 51, and 31 Å samples. Identical scans at $T = 280$ K have been subtracted to remove substrate contributions. Satellite peaks are indeed observed near their bulk positions. The symmetric splitting about the Cr(001) position shows that the Cr layers (for $t_{Cr} \gtrsim 51$ Å) form a transverse SDW with $\mathbf{Q}$ normal to the layers. No evidence of a longitudinal SDW is observed. For the 115 Å Cr sample, no magnetic scattering is observed with the scattering vector in-plane along the [100] and [010] directions, which indicates that the Cr layers are in a single $\mathbf{Q}$ configuration.

Shown in Fig. 2 are the temperature dependences of the $(0, 0, 1 \pm \delta)$ peak intensities. T_N for the Cr layers is reduced in temperature from its bulk value and depends
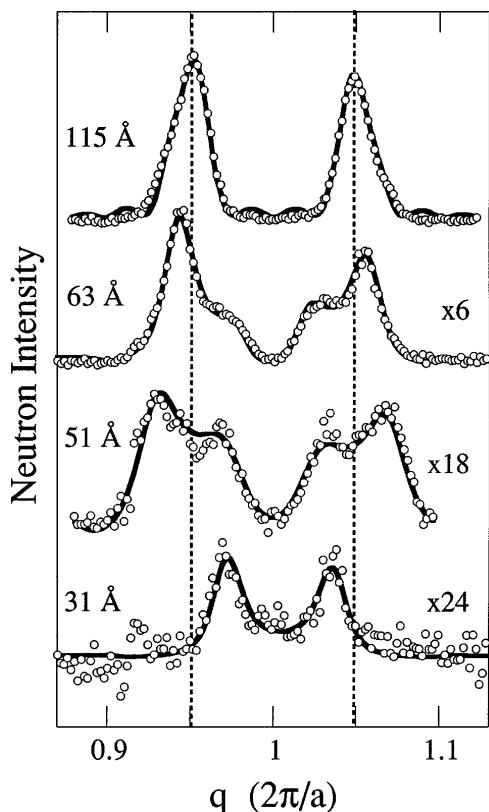
strongly on t_{Cr}. The T_N values determined from Fig. 2 are compared in the inset with the results of Ref. [13]. The T_N values are in quantitative agreement and indicate T_N is reduced as the Cr thickness approaches 42 Å. The magnetic scattering from the 44 and 31 Å samples is weak and presently precludes an accurate characterization of their temperature dependences.

The position of the magnetic peaks also depends on the Cr thickness but in a more complex manner than the T_N values. The separation of the satellite peaks for the 190 and 115 Å Cr samples is consistent with that of bulk Cr. For the 63 Å sample, the main SDW peak is shifted to a higher δ value and has additional scattered intensity close to the Cr(001) reflection. For the 51 Å sample the magnetic scattering peak is broadened and split about the expected bulk position. For the 44 and 31 Å samples two weak magnetic peaks are observed.

At first glance, the shift and splitting of the SDW peaks in the thinner Cr samples might suggest distortions of the SDW as t_{Cr} becomes comparable with the bulk SDW period or scattered intensity from different regions of the sample. However, this will be shown not to be the case, but instead results from coherent scattering of adjacent Cr layers. If each Cr layer scatters incoherently, then broad peaks located at $(0, 0, 1 \pm \delta)$ with $\xi_m \approx t_{Cr}$ will be observed. However, we find that $\xi_m > t_{Cr}$ for all samples. ξ_m values, estimated via Scherrer's equation, are 180, 260, 100, and 150 Å for the 115, 63, 51, and 31 samples, respectively. Since $\xi_m > t_{Cr}$ adjacent Cr layers scatter coherently, and interference effects need to be considered. For a perfect superlattice, instrument-resolved Bragg peaks are expected with the positions determined solely from the superlattice periodicity Λ [located at $q = na/\Lambda$ (in units $2\pi/a$)]. The SDW ordering within the Cr layers only modulates the intensities of these peaks, thus the SDW period cannot be determined directly from the peak positions. Similar observation of coherent magnetic scattering have been observed by neutron scattering for a number of rare-earth superlattices [18].

To fit the scattered intensities we use a Hendricks-Teller approach to model the superlattice [19,20]. We assumed the Cr layers have an AF-SDW order and the Fe layers are ferromagnetically ordered. The Fe and Cr layers are described by the magnetic scattering factors

$$F_{Cr}(q) = \sum_{n=0}^{N-1} (-1)^n p_{Cr} \sin(2\pi n d_{Cr}/P + \Phi)$$
$$\times \exp(iq n d_{Cr}), \tag{1}$$

$$F_{Fe}(q) = \sum_{n=0}^{M-1} p_{Fe} \exp(iq n d_{Fe}),$$

where $N(M)$ is the number of Cr (Fe) atomic planes with a lattice spacing of d_{Cr} (d_{Fe}) within a Cr (Fe) layer, and Φ and P are the phase and period of the SDW, respectively. p_{Cr} and p_{Fe} are the magnetic form factors for Cr and Fe [21], respectively, which are in proportion to their

FIG. 1. Neutron diffraction results for $[\text{Fe}(14 \text{ Å})/\text{Cr}]_N$ superlattices measured at 20 K. Cr thicknesses are listed to the left of the spectra. The spectra are offset and the scale factor to the right indicates the relative intensities normalized to the counting time and total Cr thickness. The open circles are the measured intensities, and the solid lines are calculated intensities described in the text. Parameters for the calculated intensities are given in Table I. The vertical dashed lines indicate the expected $(1 + \delta)$ and $(1 - \delta)$ satellite positions for bulk Cr at 20 K.

TABLE I. Fitting results for the $[Fe(14 \text{ Å})/Cr(t_{Cr})]_N$ superlattices shown in Fig. 1 measured at $T < 30$ K. The layer thicknesses were confined to ± 1 ML of those determined from x-ray diffraction. The bulk value for d_{Cr}, d_{Fe} and the SDW period are 1.442, 1.433, and 59 Å, respectively. The 31 Å data were fitted assuming a commensurate AF structure.

Nominal t_{Cr} (Å)	t_{Cr} (ML)	t_{Fe} (ML)	d_{Cr} (Å)	d_{Fe} (Å)	SDW period (Å)	Φ
31	22	9.3	1.440 ± 0.003	1.43[a]	$\cdots$	$\cdots$
51	36	9.4	1.445 ± 0.003	1.45 ± 0.03	60 ± 5	2.2 ± 0.4
63	43.8	9.3	1.446 ± 0.003	1.42 ± 0.03	61 ± 5	-0.1 ± 0.3
115	80	9.9	1.445 ± 0.003	1.44 ± 0.03	58 ± 4	0.0 ± 0.5
190	131[a]	9.5[a]	1.446 ± 0.003	1.44[a]	59 ± 3	0.0[a]

[a]Parameters which could not be determined in the fitting procedure and were fixed.

magnetic moments. In this simple model, all Cr layers are assumed to order identically and are separated by the Fe layers. The fitting parameters are (i) the layer thicknesses t_{Cr} and t_{Fe} (ii) the Fe and Cr lattice spacings, (iii) the period and phase of the Cr SDW, and (iv) the ratio of the Fe and Cr moments. The Fe and Cr layer thicknesses were confined in the fitting procedure to be within ± 1 ML of the values determined from the x-ray diffraction results with the bilayer period fixed to the value determined by x rays. Interfacial roughness is introduced by ensemble averaging 1 ML fluctuations in the Cr and Fe layer thicknesses, as outlined in Ref. [19]. The instrumental resolution is also included in the calculation.

The thick solid lines in Fig. 1 are the results of the fitting procedure. This simple model is able to reproduce the shift and splitting of the SDW peaks and quantitatively fits both the relative intensities and linewidths of the experimental data. For the $t_{Cr} \leq 63$ Å samples, the spitting of the peaks results from the superlattice periodicity. The Cr buffer layer represents only 1% of the Cr content of the film and does not contribute to the observed scattering. The linewidths are determined solely from the 1 ML thickness fluctuations introduced into the calculation. The fitting parameters are given in Table I, and the magnetic
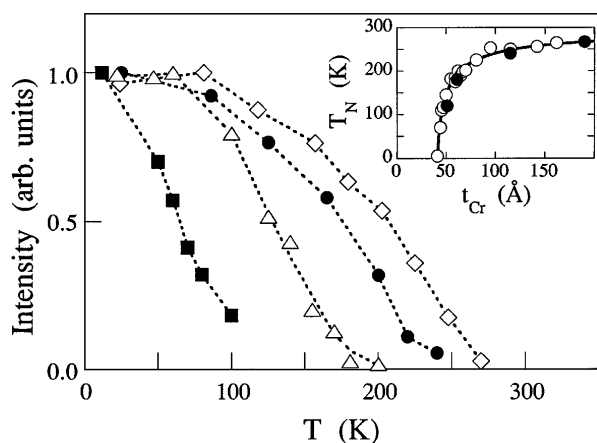
moment distributions determined from the fits are shown schematically in Fig. 3. Unlike T_N, which is strongly thickness dependent, the period of the SDW is independent of t_{Cr} and in agreement with that for bulk Cr. This even holds for the 51 Å Cr sample which only supports a half period of the SDW, and for which T_N is only 37% of the bulk value. This all suggests that the changes in T_N are not a result of impurities or strain, which would alter the Fermi surface and, therefore, the SDW period [1,22], but instead arise from a combination of finite-size effects within the Cr layers and spin-frustration effects at the Fe-Cr interface as was previously proposed [13].

The best fit value for the SDW phase suggests that the SDW orders symmetrically in the Cr layers with the nodes near the Fe-Cr interface (see Fig. 3) [23]. This behavior can be qualitatively understood from theoretical calculations of Cr ordering on stepped or interdiffused surfaces where magnetic frustration can strongly suppress the Cr moments [9]. Nodes in the SDW near the Fe-Cr interface may isolate the Cr layer from the frustrated interfaces. Such a model also explains the onset of AF-ordering transition for $t_{Cr} \approx 42$ Å, as observed in superlattices [13].

FIG. 2. Temperature dependence of the $(0, 0, 1 \pm \delta)$ magnetic peak intensities: 190 Å (open diamonds), 115 Å (filled circles), 63 Å (open triangles), and 51 Å (filled squares) samples. The inset shows T_N values determined for these samples (filled circles) compared to the results of Ref. [12] (open circles). The lines are guides to the eye.
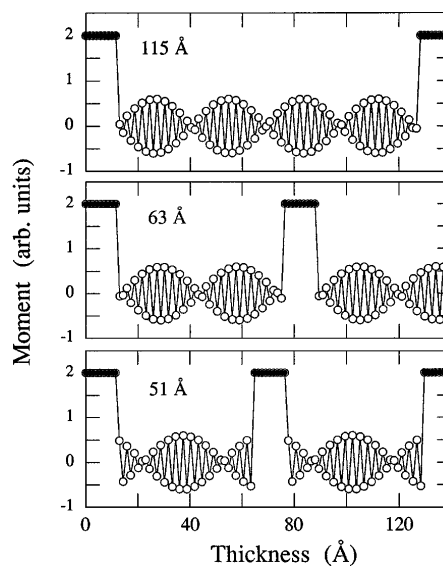

FIG. 3. Schematic representation of the magnetic moments for Fe and Cr layers determined from the fitting results of Fig. 1 and Table I for the 115, 63, and 51 Å samples. The filled circles indicate the Fe moments and the open circles the Cr moments.

If at least a half period of the SDW (≈ 30 Å) is required to sustain homogeneous AF order in the Cr layer, and the nodes are located 4 ML from the interface, a minimum Cr thickness ≈ 41 Å is then required to sustain AF-SDW order, in close agreement with experimental results. This is consistent with results of Ref. [2] which identify periodic phase slips in the Cr ordering for Cr thicknesses of 24, 44, and 64 ML. This suggests that the first phase slip (or node in the SDW) occurs near the interface at a Cr thickness of 4 ML. In Ref. [3], imaging of the Cr ordering near the Fe-Cr interface shows irregularities for the first three ML of Cr resulting from interdiffusion [15] before AF ordering begins at the fourth ML.

Although the scattered intensity is weaker for thinner Cr layers, and previous magnetic and transport studies failed to see any signatures of a Néel transition for $t_{Cr} < 42$ Å, there still is magnetic scattering from the 31 Å sample (see Fig. 1). The scattering persists up to at least $T = 175$ K (above T_N of the 51 Å Cr samples) and consists of two sharp peaks about the Cr(001) and a broad diffuse component centered near the Cr(001) reflection. The scattering can be quantitatively fitted assuming a commensurate AF structure (see Fig. 1). The observe splitting of the peaks results from the superlattice periodicity ($\Delta q = a/\Lambda$), and cannot be interpreted as arising from SDW order. The low intensity of the 31 Å sample may be interpreted as arising from a combination of (i) magnetic ordering of only a small region of the sample, (ii) a reduced Cr moment, or (iii) inhomogeneous ordering (AF domains), which results in a small average moment for a given atomic plane. The first is unlikely given the coherent nature of the scattering. Separating the latter two is difficult in a scattering experiment since the average structure is measured and a local probe of the Cr moment is required. However, the presence of broad diffuse scattering is consistent with domain formation, which is expected for commensurate AF order if the Cr layer can be described by terraces separated by monoatomic steps. This model was suggested by Slonczewski [12] as a mechanism to explain the biquadratic interlayer coupling in Cr and Mn [24] spacers. For thicker Cr layers, the presence of nodes may relieve the interfacial frustration, resulting in homogeneous AF-SDW ordering and suppression of this contribution to the biquadratic coupling for $T < T_N$ [13].

Finally, it is somewhat surprising to observe coherent scattering of adjacent Cr layers in all the samples. In the intensity calculations, increasing the fluctuations of either the Cr or Fe layer thicknesses to greater than 1 ML is sufficient to suppress the coherent scattering. The high degree of order suggested by these calculations is not expected for superlattices, and furthermore, x-ray results suggest roughnesses >1 ML. However, x-ray scattering measures the *structural* order, whereas the present neutron results are probing the *magnetic* order. If the lateral ξ_m is large compared with the structural disorder, the magnetic ordering may be insensitive to local imperfections of the interface [25].

In summary, we have investigated the AF-SDW order of Cr layers in Fe/Cr(001) superlattices by neutron scattering. T_N is strongly thickness dependent in agreement with previous magnetic and transport results [13]. For $t_{Cr} \gtrsim 51$ Å, we find a transverse SDW is formed for all temperatures below T_N with a single **Q** normal to the layers. The observed SDW period is close to the bulk value. For the $t_{Cr} = 31$ Å, the magnetic scattering can be described by commensurate AF order. A coherent magnetic structure is formed with the magnetic coherence length greater than the Cr layer thickness and the nodes of the SDW near the Fe-Cr interfaces.

[1] E. Fawcett, Mod. Phys. **60**, 209 (1988).
[2] J. Unguris, R. J. Celotta, and D. T. Pierce, Phys. Rev. Lett. **69**, 1125 (1992).
[3] D. T. Pierce, R. J. Celotta, and J. Unguris, J. Appl. Phys. **73**, 6201 (1993).
[4] T. G. Walker *et al.,* Phys. Rev. Lett. **69**, 1121 (1992).
[5] F. U. Hillebrecht *et al.,* Europhys. Lett. **19**, 711 (1992).
[6] Y. U. Idzerda *et al.,* Phys. Rev. B **48**, 4144 (1993).
[7] C. Turtur and G. Bayreuther, Phys. Rev. Lett. **72**, 15 571 (1994).
[8] A. Vega *et al.,* Phys. Rev. B **51**, 11 546 (1995).
[9] D. Stoeffler and F. Gautier, J. Magn. Magn. Mater. **147**, 260 (1995).
[10] P. Grünberg *et al.,* Phys. Rev. Lett. **57**, 2442 (1986).
[11] B. Heinrich and J. F. Cochran, Adv. Phys. **42**, 523 (1993).
[12] J. C. Slonczewski, Phys. Rev. Lett. **67**, 3172 (1991); J. Magn. Magn. Mater. **150**, 13 (1995).
[13] E. E. Fullerton *et al.,* Phys. Rev. Lett. **75**, 330 (1995).
[14] J. Meersschaut *et al.,* Phys. Rev. Lett. **75**, 1638 (1995).
[15] D. Venus and B. Heinrich, Phys. Rev. B **53**, R1733 (1996).
[16] E. E. Fullerton *et al.,* Phys. Rev. B **48**, 15 755 (1993); Appl. Phys. Lett. **63**, 1699 (1993).
[17] J. P. Hill, G. Helgesen, and D. Gibbs, Phys. Rev. B **51**, 10 336 (1995).
[18] C. J. Majkrzak *et al.,* Adv. Phys. **40**, 99 (1991).
[19] E. E. Fullerton *et al.,* Phys. Rev. B **45**, 9292 (1992).
[20] J. A. Borchers *et al.,* Phys. Rev. B **51**, 8276 (1995).
[21] A. J. Freeman and R. E. Watson, Acta Crystallogr. **14**, 234 (1961).
[22] P. Ponntag *et al.,* Phys. Rev. B **52**, 7363 (1995).
[23] For a Cr thickness of 51 Å it is not possible to have both the Cr SDW symmetrically ordered and the nodes located near the interface. In addition to the fits shown in Fig. 3, local minimum in the least-squares fitting procedure are possible in which the Cr layers order asymmetrically. In Fig. 3 we show the symmetric solutions.
[24] M. E. Filipkowski *et al.,* Phys. Rev. Lett. **75**, 1847 (1995).
[25] M. J. Pechan *et al.,* J. Appl. Phys. **75**, 6178 (1994).